TAS Journal, vol. 2, n. 3, p.156.
SEPTEMBER **2018**
ISSN: 2595-1521
marcelots@ipt.br

Membrane shaping by low coherence speckle interferometry for pressure measurement

Saita MT*‡, Barbosa EA*, Degasperi FT*, Wette NU§.

** Centro Estadual de Educação Tecnológica Paula Souza, São Paulo, Brasil.*

‡Instituto de Pesquisas Tecnológicas, São Paulo, Brasil.

§ Instituto de Pesquisas Energéticas e Nucleares, São Paulo, Brasil.

Abstract. In this work we developed a novel pressure measurement technique based on the deformation evaluation of a membrane submitted to a pressure differential. The deformed membrane shape was determined by low-coherence speckle interferometry. In this method, a tunable diode laser at 660 nm emitting simultaneously two or more longitudinal modes illuminates the optical setup. The resulting speckled low spatial frequency interferogram of the image corresponding to the membrane shape was evaluated by conventional 4-stepping and phase unwrapping analyses. The sensitivity of the measurement process was controlled by tuning the laser with the help of the Littman-Metcalf arrangement using a 2380 lines/mm reflective diffraction grating, which provided a tunable range of 3 nm. The 0.420 mm thick aluminum membrane was submitted to pressure values from 0 to 90 kPa and a curve of the maximum membrane deformation as a function of the pressure was obtained. The experimental results were compared with the ones obtained by a numerical algorithm.

Key-words. *Speckle, Interferometry, Deformation, Pressure.*

Introduction. Along the years the employ of interferometry for pressure measurement was proposed by several authors (1-6). Those techniques basically measure the deformation of membranes or diaphragms in the range from hundreds of micrometers up to several millimeters. In this framework we propose the deformation measurement of a membrane submitted to a pressure differential by low coherence speckle interferometry. For this purpose the interferometer is illuminated by a tunable diode laser, which allows selecting the most suitable emission parameters according to a required sensitivity (7). In addition, low coherence techniques do not require very severe stability conditions, if compared with other conventional interferometry methods (8).

TAS Journal, vol. 2, n. 3, p.157.
SEPTEMBER 2018
ISSN: 2595-1521
marcelots@ipt.br

Low coherence speckle interferometry. Objects with rough surfaces illuminated simultaneously by two laser beams with slightly different wavelengths λ_1 and λ_2 may generate an object image modulated by low spatial frequency fringes in a DSPI (Digital Speckle Pattern Interferometry) setup (9). Each contour fringe of the resulting interferogram corresponds to a plane of constant elevation. The distance between adjacent planes is closely related to the synthetic wavelength λ_S given by

$$\lambda_S = \lambda_1\lambda_2/|\lambda_1-\lambda_2| \quad (1)$$

The light intensity resulting from the interference of the studied object wave and the reference wave is recorded onto a CCD target. The background noise due to the reference beam intensity is removed with the help of the subtraction method (9), so that the contour fringe pattern intensity is given by (10)

$$I_{(x,y)} = I_0 \cos^2\left[\frac{\pi(\Gamma_{S_{(x,y)}}-\Gamma_R)}{\lambda_S}\right] \quad (2)$$

Equation (2) above was obtained considering that each laser mode has the same intensity I_0. $\Gamma_S(x,y)$ is the optical path of the object beam through a point (x,y) on the object surface and Γ_R is the reference beam path.

External cavity diode laser. According to equation (1), by properly selecting wavelengths λ_1 and λ_2 the synthetic wavelength value can be conveniently set according to the surface dimensions and geometry. Among several laser tuning methods we use the Littman-Metcalf (LM) feedback technique whose setup is shown in figure 1. This technique is based on a controlled feedback by an external cavity with a diffraction grating for emission wavelength selection and modes stabilization (11, 12).

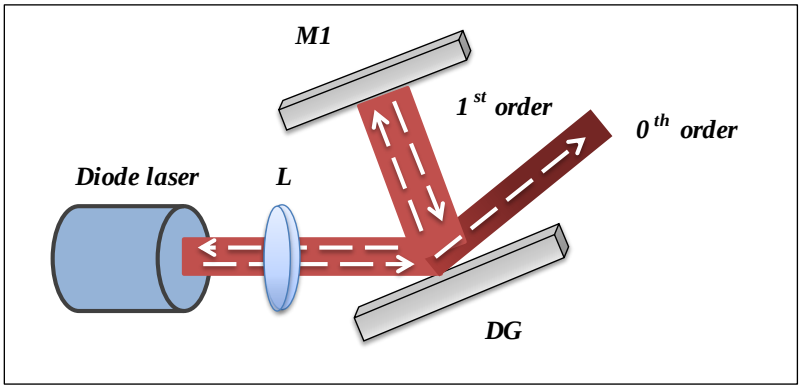

Figure 1. Littman-Metcalf optical setup.

TAS Journal, vol. 2, n. 3, p.158.
SEPTEMBER 2018
ISSN: 2595-1521
marcelots@ipt.br

The main component of the LM setup is the diffraction grating. As shown in figure 1, the 0^{th} order diffracted beam is used to illuminate the interferometer. The mode selection is made as the 1^{st} order beam is reflected by the properly adjusted mirror M1 back to the grating and consequently to the laser. Only the modes selected by M1 are reinforced inside the laser diode and have enough gain to oscillate. Thus, the spectral content of the laser inciding into the speckle interferometer is directly determined by the LM setup.

Experiments. In the proposed method, the pressure was determined by evaluating the deformation undergone by a diaphragm (or membrane) submitted to a pressure differential. Several pressure values were applied on the diaphragm and their respective deformation values were measured. By using software COMSOL Multiphysics an experimental relation between measured deformation and pressure was determined.

Figure 2 shows in detail the aluminum membrane holder. At the left illuminated face there is atmospheric air, while at the internal right side the pressure to be measured. In this configuration the device measures "gauge pressure" where positive values represents pressures above the atmospheric pressure and negative values represents pressures below the atmospheric pressure (13).

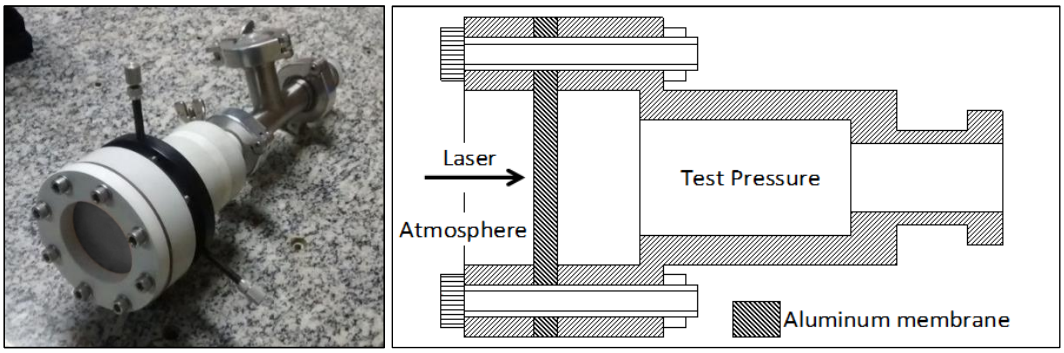

Figure 2. Membrane assembly.

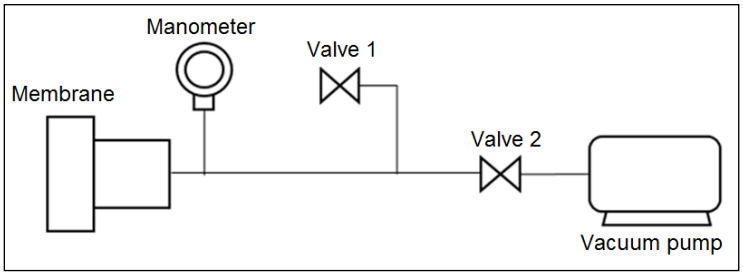

Figure 3. Vacuum pump.

TAS Journal, vol. 2, n. 3, p.159.
SEPTEMBER 2018
ISSN: 2595-1521
marcelots@ipt.br

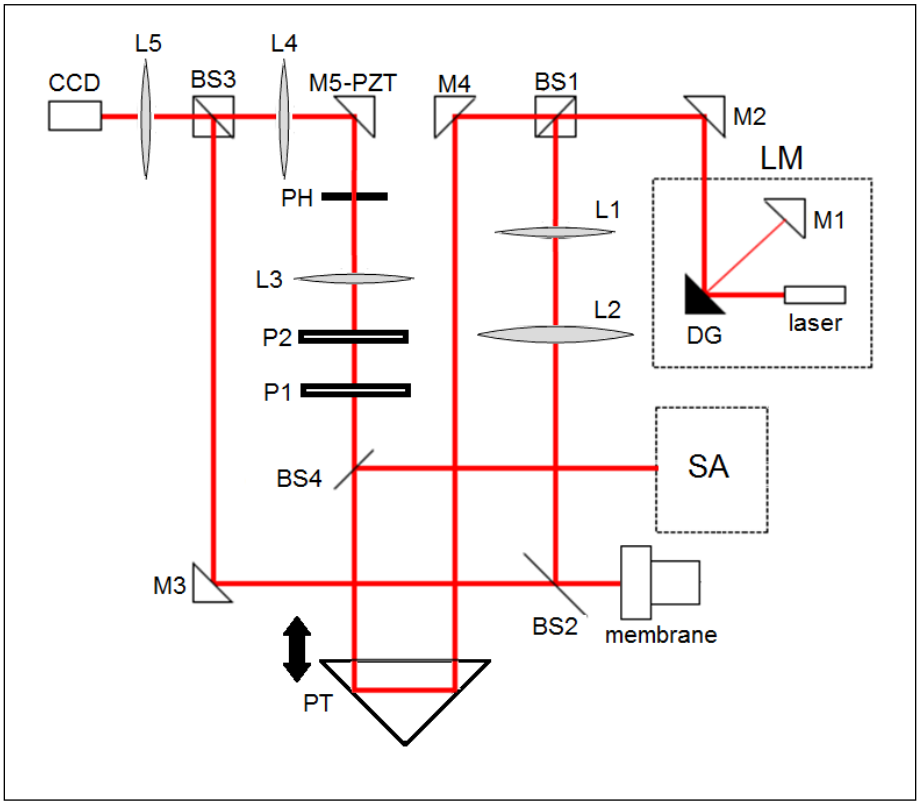

Figure 4. Optical setup: M1 to M5, mirrors; L1 to L5, lenses;

In the speckle interferometer the beam leaves de LM arrangement and is divided by reference and object arms at beam splitter BS1. In the object arm, the beam is collimated by lenses L1 and L2, hits the object after passing through beam splitter BS2. The light scattered by the membrane passes through mirror M3 and beam splitter BS3, and the membrane image is formed at the 15-μm pixel size CCD camera by lens L5.

At the left BS2 side the reference beam passes through a 90-degree prism translator PT, which can be translated (see fig. 4) with the help of a micrometric screw, not shown in figure 4, in order to perform the 4-stepping procedure (9). After being reflected by PT, the beam passes through polarizers P1 and P2 for intensity selection and pinhole PH for beam spatial filtering. Lenses L4 and L5 collimate the reference beam to interfere with the object beam at the CCD target. Mirror M5-PZT is supported by a piezoelectric ceramic vibrating at 5 Hz in order to perform the subtraction method for fringe visibility enhancement (9). At beam splitter BS4 the beam is partially deviated to allow real time spectrum monitoring at the home-made spectrum analyzer SA.

TAS Journal, vol. 2, n. 3, p.160.
SEPTEMBER 2018
ISSN: 2595-1521
marcelots@ipt.br

Experimental results.

Fringe evaluation – As an example, figure 5 shows a sequence of four frames comprising a complete set of interferograms which are sequentially π/2-shifted for a given membrane deformation. The concentric circular fringes in those frames show clearly that the maximum deformation was achieved at the central part of the membrane. Figure 6a shows the resulting phase map and figure 6b shows the unwrapped phase of the membrane. The darker the gray level, the lower the vertical displacement of a point on the membrane. Again, figure 6b shows that the darkest central region of the membrane corresponds to its largest deformation. For each pressure differential applied to membrane, a set of four frames like the one of figure 5 and a phase map and an unwrapped phase like the ones of figure 6 were obtained. After converting the gray levels of the unwrapped phase into height coordinate values, one obtains a deformation map of the surface.

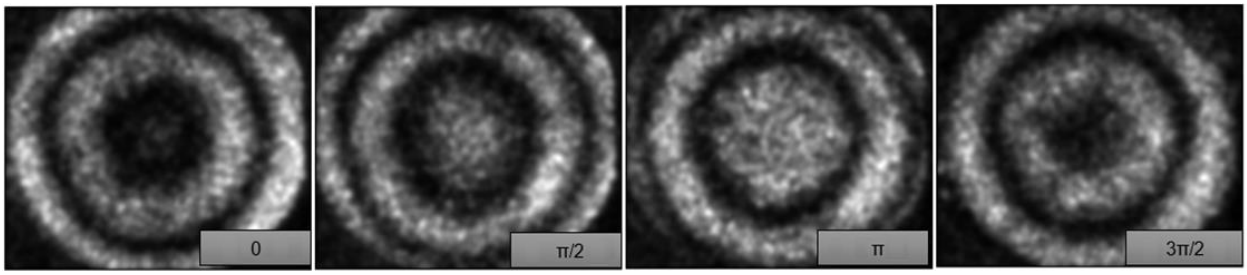

Figure 5. π/2-shifted 4-stepping interferograms.

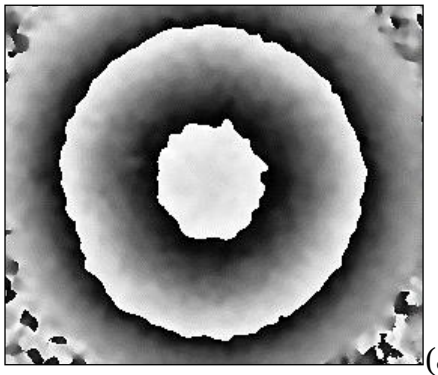
(a)
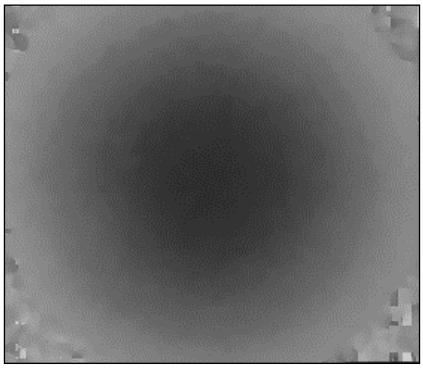
(b)

Figure 6. a – Phase mapping; b – unwrapped phase.

Deformation measurement – Table 1 shows the relevant material and dimensional properties of the aluminum alloy used in the numerical calculations. The average membrane thickness is (423 ± 3) μm and its diameter is (55.00 ± 0.04) mm.

TAS Journal, vol. 2, n. 3, p.161.
SEPTEMBER 2018
ISSN: 2595-1521
marcelots@ipt.br

Table 1. Mechanical properties of the aluminum alloy (14)

Material	Elasticity modulus	Poisson Coefficient	Thermal expansion
Aluminium alloy	72 GPa	0,33	23,5 µ/°C

Figure 7 shows the experimental values of maximum deformation undergone by the membrane and compare them with values numerically obtained by the software COMSOL Multiphysics (version 5.1). For each pressure value, the input dada for the numerical calculation were obtained from table 1.

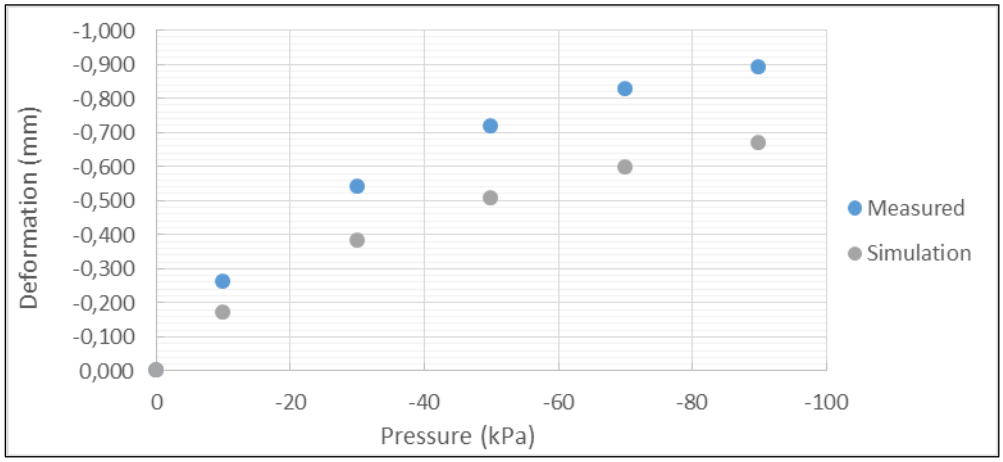

Figure 7. Maximum deformation of the membrane submitted to the pressure differential. Blue circles, experimental results obtained from low coherence speckle interferometry; gray circles, numerical results.

Conclusion. The membrane deformation was successfully measured by the proposed optical arrangement and the experimental results were compared with a numerical simulation. The experimental results presented a deviation from the numerical algorithm, however both curves show similar behavior to the application of pressure. The found errors could be related to a systematic deviation in the determination of the synthetic wavelength or to a difference between the mechanical properties of the aluminum alloy used and values obtained from the literature. As a suggestion to future works, the authors propose the creation of an uncertainty model for the measurements to improve the analysis of the results.

References.

(1) Benaissa K, Nathan A, IC compatible optomechanical pressure sensors using Mach-Zehnder interferometry. IEEE transactions on Electron Devices 1996, (1571-1582) :43 – 9.

(2) Huntley J M, Saldner H O, Multi-channel pressure sensor using speckle interferometry. Optics Las Engng 1995; (263-275): 23 - 5.

(3) Li M; Wang M, Li H, Optical MEMS pressure sensor based on Fabry-Perot interferometry. Opt. Express 2006; (1497-1504):14- 4.

(4) Pang C, Bae H, Gupta A, Bryden K, Yu M, MEMS Fabry-Perot sensor interrogated by optical system-on-a-chip for simultaneous pressure and temperature sensing. Opt. Express 2013; (21829-21839):21-19.

(5) Torres FJ, Application of digital holographic interferometry to pressure measurements of symmetric, supercritical, and circulation control airfoils in transonic flow fields. Proceedings of High speed photography, videography, and photonics IV; 1986. International Society for Optics and Photonics.

(6) Totsu K, Haga Y, Esashi M. Ultra-miniature fiber-optic pressure sensor using white light interferometry. Journal of Micromechanics and Microengineering 2004; (71): 15-1.

(7) da Silva DM, Barbosa EA, Wetter NU. Real-time contour fringes obtained with a variable synthetic wavelength from a single diode laser. Applied Physics B 2015;(159-166):118 - 1.

(8) Francis D et al. A mechanically stable laser diode speckle interferometer for surface contouring and displacement measurement. Measurement Science and Technology 2015; (055402): 26 - 5.

(9) Hack E, Frei B, Kästle R, Sennhauser U, Additive-subtractive two-wavelength ESPI contouring by using a synthetic wavelength phase shift, Appl. Opt. 1998; (2591–2597):37.

(10) Barbosa EA, Lino ACL. Multiwavelength electronic speckle pattern interferometry for surface shape measurement. Appl. Opt. 2007; (2624-2631): 46 -14.

(11) Littman MG, Metcalf HJ, Spectrally narrow pulsed dye laser without beam expander. Appl. Opt. 1978;(2224-2227): 17-14.

(12) Liu K; Littman M G. Novel geometry for single-mode scanning of tunable lasers. Opt. Lett 1981; (117-118): v. 6-3.

(13) Cusco, L. et al. Guide to the Measurement of Pressure and Vacuum. The Institute of Measurement and Control, London, 1998.

(14) Young WC; Budynas RG. Roark's formulas for stress and strain. 7 ed. New York: McGraw-Hill, 2002.